Analytica Chimica Acta 1000 (2018) 232–238

Contents lists available at ScienceDirect

Analytica Chimica Acta

journal homepage: www.elsevier.com/locate/aca

3D capillary stop valves for versatile patterning inside microfluidic chips

V.A. Papadimitriou*, L.I. Segerink, A. van den Berg, J.C.T. Eijkel

BIOS-Lab on a Chip Group, MESA+ Institute of Nanotechnology, MIRA Institute for Biomedical Technology and Technical Medicine, Max Planck - University of Twente Center for Complex Fluid Dynamics, University of Twente, The Netherlands

HIGHLIGHTS

- Capillarity-based technique for patterning antibodies in closed chips.
- Antibody deposition *after* chip bonding.
- Technique based on 3D capillary valving.
- Robust micromachining methods allowed.

GRAPHICAL ABSTRACT

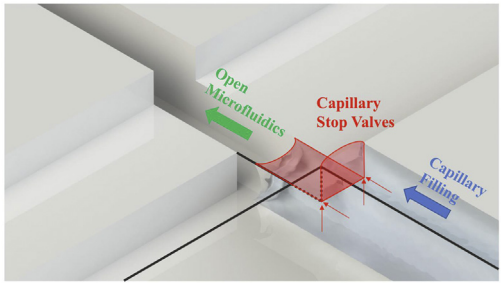

ARTICLE INFO

Article history:
Received 13 November 2017
Received in revised form
20 November 2017
Accepted 22 November 2017
Available online 25 November 2017

Keywords:
Capillary patterning
3D capillary valves
Antibody coating
Closed-chip

ABSTRACT

The patterning of antibodies in microfluidics chips is always a delicate process that is usually done in an open chip before bonding. Typical bonding techniques such as plasma treatment can harm the antibodies with as result that they are removed from our fabrication toolbox. Here we propose a method, based on capillary phenomena using 3D capillary valves, that autonomously and conveniently allows us to pattern liquids inside closed chips. We theoretically analyse the system and demonstrate how our analysis can be used as a design tool for various applications. Chips patterned with the method were used for simple immunodetection of a cardiac biomarker which demonstrates its suitability for antibody patterning.

1. Introduction

Proteomic studies by specific protein-antibody binding have a wide range of applications, from early diagnosis of diseases to fundamental medical and biological studies. Microfluidic chips offer an attractive platform for these studies for various reasons such as the use of extremely low volumes of expensive samples, chemicals and reagents used in immunodetection. For such studies it is necessary to coat a section of the chip with the protein-binding molecules, often an antibody [1]. Typically, first one part of the device is coated with the antibody and then bonded to create the microfluidic chip [2]. There are several methods for patterning antibodies prior to bonding with the most widely used ones being bioprinting [3] and light assisted immobilization [4]. However, when the antibody coating is performed before the final chip is bonded (open-chip), any fabrication process that can harm the antibody coating (e.g. high temperature, plasma and ultraviolet (UV) treatment) is prohibited. Use of less stable materials (such as

* Corresponding author.
E-mail address: v.papadimitriou@utwente.nl (V.A. Papadimitriou).

https://doi.org/10.1016/j.aca.2017.11.055

polydimethylsiloxane (PDMS)) or more delicate bonding methods then becomes necessary. Such bonding methods could be gluing, use of pressure sensitive adhesive (PSA) tapes [5] and use of chemical functionalized surfaces [6]. As also these methods have their limitations, there exists a need for an antibody immobilization method that can be used *after* chip bonding. Trapping of antibody labelled beads for immonudection in closed chip has been previously reported [7] but bead trapping lacks the flexibility of patterning shapes. Capillary filling methods are an excellent candidate for this. The use of capillary effects has always been popular in microfluidic systems [8]. Specifically, the passive handling of fluids provided by the capillary phenomena simplifies the device operation and minimizes the need of external actuation devices (e.g. pumps) which makes the resulting devices inherently simple to use without any training [9]. Devices based on capillary system have found applications such as diagnostics in 'autonomous' systems with sequential transport of minute amounts of liquids [10], capillary pinning of hydrogels [11] and phase-guides for passive routing of liquids [12].

Here we develop a method based on capillarity to passively pattern antibodies in a closed, bonded chip (Fig. 1). This method solves the bonding issue mentioned above, and consequently puts all the reliable but "harsh" fabrication processes back into our fabrication toolbox, allowing the use of stable microfluidic devices.

2. Theory

The configuration we propose for capillary patterning uses a series of capillary stop valves [13] in 3D configuration (Fig. 2). The first stop valve is formed when a deep channel intercepts another shallower channel. A liquid is applied to the deep channel and fills it via capillary forces. Subsequently, when it reaches the intersection, the part of the liquid that meets the abrupt opening will become pinned, similar to the traditional 2D capillary stop valves. However, the part of the liquid that contacts the shallow channel in a ditch on the bottom of the intersecting channel can flow freely across this channel. The liquid is now pinned in the perpendicular direction as it crosses the channel and fills the ditch. When the liquid has crossed the entire shallow channel, it will fully wet the deep channel on the opposite side, being pinned again in the perpendicular direction to the shallow ditch as on the other side.

The 3D capillary valve pattern we use has three distinct regions

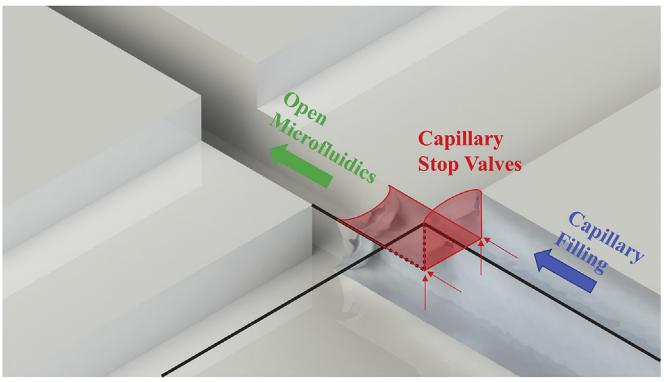

Fig. 2. Three different capillary phenomena that are exploited by the 3D valves. Capillary filling moves the liquid towards the valve. Capillary stop valves pin the liquid in two directions marked with red arrows (the pinned liquid air interface is shaded with red color) and the liquid advances via an open microfluidic structure. The dimensions of the deep channel are 75 μm in depth and 10 μm in width and the shallow channel 35 μm deep, creating an open microfluidic feature with depth of 40 μm. The width of the shallow channel is not critical to the functionality of the device as it will be explained later. (For interpretation of the references to colour in this figure legend, the reader is referred to the web version of this article.)

where three different capillary phenomena take place: a) capillary filling, b) capillary pinning (stop valve), c) open microfluidics (Fig. 2) [14]. Each of them will be investigated independently.

All three different capillary phenomena are governed by the liquid pressure that is generated during the filling process of the chip. Following the analysis by Man et al. [13], the liquid pressure at the meniscus during filling can be derived as the change of total interfacial energy on an increase of the filling liquid volume,

$$P = \frac{dU_t}{dV} \tag{1}$$

Here P [Pa] is the pressure across the liquid/air interface, U_t is the total interfacial energy [J], and V [m^3] is the volume of the liquid in the chip. The total interfacial energy is given by equation (2),

$$U_t = A_{sl}\gamma_{sl} + A_{sg}\gamma_{sg} + A_{lg}\gamma_{lg} \tag{2}$$

where A is surface area of each interface and γ is the energy per unit

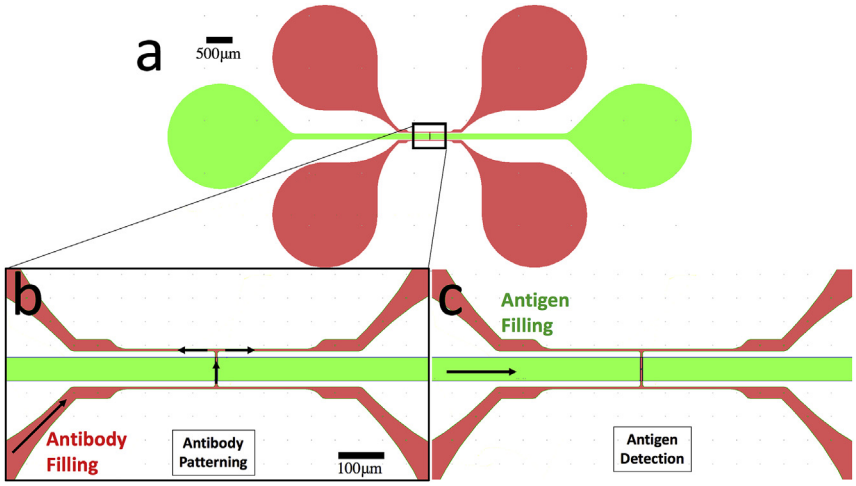

Fig. 1. a) Typical outline of device. The red (deeper) channel is dedicated for the capillary patterning of antibodies. Where the green (shallower) channel is dedicated for the antigen containing sample. b) Introduction of a droplet of antibody solution to one of the red reservoirs and capillary filling of the 3D valve. After incubation of the antibody the red channel is flushed. c) Transport through the main channel (green) of the fluorescent antigen-containing solution. (For interpretation of the references to colour in this figure legend, the reader is referred to the web version of this article.)

area of that interface (interfacial tension). The subscripts s, l, g stand for solid, liquid and gas, e.g. A_{sl} is the surface area between solid and liquid phase, i.e. the wetted area of the channel. Equation (2) simply describes the sum of all interfacial energies. Depending on the balance of those energies either a negative or positive total energy change at a liquid volume can occur. A negative energy change results in a lower pressure in respect to the atmospheric pressure which leads to capillary filling, and a positive energy change results in a positive pressure which leads to liquid pinning. We can rewrite equation (2) by using Young's equation (3) that relates interfacial tensions by the advancing liquid/air contact angle θ,

$$\gamma_{sl} = \gamma_{sg} - \gamma_{lg}\cos\theta \tag{3}$$

By combining equations (2) and (3) we obtain

$$U_t = (A_{sl} + A_{sg})\gamma_{sg} - A_{sl}\,\gamma_{lg}\,cos\theta + A_{lg}\,\gamma_{lg} \tag{4}$$

$$U_t = U_0 - \gamma_{lg}\left(A_{sl}\,cos\theta - A_{lg}\right) \tag{5}$$

where $U_0 = (A_{sl} + A_{sg})\gamma_{sg}$ is constant because the total area of solid is constant.

Substituting equation (5) in equation (1) we obtain the general expression for the meniscus pressure,

$$P = \frac{dU_t}{dV} = -\gamma_{lg}\left(cos\theta\,\frac{dA_{sl}}{dV} - \frac{dA_{lg}}{dV}\right) \tag{6}$$

Equation (6) will be used to calculate the meniscus pressure in the three distinct regions of the device. This pressure is the driving force which will either pin the liquid or passively fill the device. The pressure at the reservoir is equal to atmospheric pressure but we will arbitrarily define it as zero for a more intelligible analysis; hence a negative pressure translates to passive filling and a positive pressure to liquid pinning.

2.1. Capillary filling

At the start of the filling process the liquid fills a rectangular channel of constant cross-sectional area. In that case $A_{lg} = wh$ in equation (6) will be constant when the liquid invades (assuming a flat meniscus), so that $dA_{lg}/dV = 0$. Furthermore $dA_{sl} = 2(w+h)dL$ and $dV = wh\,dL$, where w, h, L are the width, height and length of the wetted channel. As a result equation (6) for the meniscus pressure reduces to

$$P = -\gamma_{lg}\left(2cos\theta\frac{h+w}{wh}\right) \tag{7}$$

hence a negative constant pressure at the front of the meniscus is pulling the liquid through the channel. As the liquid advances and wets a bigger part of the channel, the hydraulic resistance increases linearly with filled channel length (assuming a constant channel cross-section area) and since the filling is driven by constant pressure the flow rate will decrease with the square root of time. In typical cases filling will eventually stop when the liquid becomes pinned at a small asperity. In our device during the entire filling process the pressure is sufficiently negative and the hydraulic resistance small enough for the liquid to move very rapidly (flow velocity in the range of millimeters per second, see ESI). After filling the rectangular channel, the liquid reaches the next region of the device, where the top part of the liquid meets a capillary valve and the bottom part an open microfluidic channel (Fig. 2).

2.2. Capillary stop valve

The top part of the liquid meets an abrupt expansion of the channel, i.e. a geometrical capillary stop valve [13] (indicated in red in Fig. 2). Capillary stop valves have been extensively studied and a first 2D model was made by Man et al. [13] where the pressure barrier and the energy of such system was calculated with the use of equations (6) and (2) and the geometrical change of the meniscus curvature. They showed that the pressure barrier in such a valve equals to:

$$\Delta P = \frac{2\gamma_{la}}{w}\left(\frac{\cos\theta - \frac{\alpha}{\sin\alpha}}{\frac{1}{\sin\alpha}\left(\frac{\alpha}{\sin\alpha} - \cos\alpha\right)}\right)$$

Where α is the meniscus arc angle (see Fig. 3).

For a pressure barrier of zero the critical expansion angle (β_c), i.e. the minimum expansion angle needed to achieve pinning, can be calculated and it is given by:

$$\beta_c = \frac{\pi}{2} - \theta \tag{8}$$

Later more sophisticated 3D models were proposed [15,16] where the pressure barrier is given by:

$$\Delta P = -\frac{2\gamma_{la}\left[\left(\frac{w\cos\theta}{\cos\beta}\right) + h + h\left(\frac{\tan\beta}{\sin\alpha_h}\right)\left(\frac{\alpha_h}{\sin\alpha_h} - \cos\alpha_h\right) - \left(\alpha_h\alpha_v w\frac{\tan\beta}{\sin\alpha_h\sin\alpha_v}\right)\right]}{w\left[h - \left(h\frac{\tan\beta}{\sin\alpha_h}\right)\left(\frac{\alpha_h}{\sin\alpha_h} - \cos\alpha_h\right) - \left(\frac{w\tan\beta\alpha_h}{2\sin\alpha_h\sin\alpha_v}\right)\left(\frac{\alpha_v}{\sin\alpha_v} - \cos\alpha_v\right)\right]} \quad [16] \tag{9}$$

Here α_h and α_v is the horizontal and vertical arc angle of the meniscus respectively, w is the width of the valve before the expansion, h its height, and finally β is the expansion angle (Fig. 3).

2.3. Open microfluidics

After the stop valve, the liquid now will proceed by filling an open channel, crossing the bottom of a wider channel (indicated in

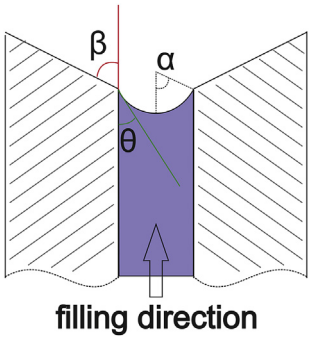

Fig. 3. Typical layout of a 2D capillary stop valve.

green in Fig. 2). This geometry is known as open microfluidics, a concept introduced by the Beebe group [14]. Also in this case, the condition for passive filling is a negative pressure at the meniscus relative to the reservoir pressure (defined as 0 bar). From equation (6) a negative pressure condition (relative to reservoir) translates to:

$$\cos\theta > \frac{dA_{lg}}{dA_{sl}} \tag{10}$$

Equation (10) gives the general condition for passive filling of an open microfluidic feature of arbitrary shape. When we assume liquid interfaces with no curvature, equation (10) is simplified to:

$$\cos\theta > \frac{p_{lg}}{p_{sl}} \tag{11}$$

where p_{sl} is the perimeter of the cross section of the channel that is wetted, and p_{lg} is the non-wetted one. For the simple case of a rectangular channel with three walls we can calculate the meniscus pressure in a similar fashion as in equation (7) as

$$P = -\gamma_{lg}\left(cos\theta\frac{2h+w}{wh} - \frac{1}{h}\right) \tag{12}$$

Once again, the flow in this simple open channel geometry is caused by a constant negative pressure (relative to reservoir pressure) at the proceeding liquid front. Similar to the capillary filling the flow rate will reduce as the liquid proceeds because of the pressure drop arising from the increasing hydraulic resistance. In open microfluidics as in closed-channel microfluidics the distance travelled by the invading liquid scales with the square root of time [17]. In our system the resistance of the open microfluidic channels is low as they are short (up to 100 μm straight channel) and the meniscus pressure low, resulting in a capillary filling velocity in the range of millimeters per second which ensures the successful filling of the open microfluidic structure. Following the openmicrofluidics section, the liquid will proceed filing the closed microfluidic channel at the other side of the channel it just crossed.

3. Experimental

In order to test the geometry proposed in Fig. 2, chips where fabricated out of PDMS with standard soft lithography methods [18]. Specifically, a silicon wafer was dehydrated on a hotplate 120 °C for 5min and a layer of Microchem SU-8 2050 negative photoresist was spin-coated with a thickness of 35 μm. Soft bake, UV exposure (photolithography with the blue pattern of Fig. 4 as mask), hard bake and resist development were performed according to the fabrication parameters suggested by the photoresist manufacturer. The same process was repeated for a second layer of SU-8 with a thickness of 75 μm, using the green pattern of Fig. 4 as a photolithography mask. The silicon wafer with the patterned SU-8 was then used as a template for the soft lithography of PDMS. The obtained PDMS chips were bonded on standard microscope glass slides after O_2 plasma treatment and left in the oven at 60 °C for varying amounts of time depending on the application, in order to reduce their hydrophilicity. Specifically for the characterization device with water/water mixtures the PDMS chips were annealed for 5 h. For the immunodetection application were aqueous solutions are used, the chips were annealed for 90 min. PDMS was chosen because its surface properties are well investigated [19,20] and can be trivially tuned via O_2 plasma treatment. In addition to the simple straight channel geometry, various other channel geometries shown in Fig. 4a–i were tested in order to test the capabilities of the capillary patterning procedure.

For the immunodetection experiments, chips were fabricated out of PDMS as described before and bonded to standard microscopy slides. A droplet of an aqueous antibody coating solution (5 μg/ml Anti-Cardiac Troponin I antibody (Abcam) in carbonate/bicarbonate buffer pH 9.2) was introduced in the antibody designated inlet channel after which via capillary forces the bottom of the sample channel was patterned. The antibody coating solution was allowed to bind for 15min and then the chip was flushed with 1xPBS (Sigma-Aldrich) + 0.1% Tween 20 (Sigma-Aldrich) solution and subsequently with DI water and dried overnight. To demonstrate proper functioning of the device as a protein sensor, fluorescently labelled Cardiac troponin-I (Abcam, 2.2 μg/ml) in 1xPBS + 1% BSA (Sigma-Aldrich) was introduced in the sample channel and allowed to incubate for 15min, after which the channel was flushed with 1xPBS+ 0.1% Tween and the fluorescence emission recorded. Cardiac troponin-I was chosen as the target protein because it is a key biomarker for cardiac disease.

4. Results and discussion

4.1. Characterize device operation using ethanol/water mixtures

As shown in the theoretical section, the liquid/air interfacial tension (γ_{sg}) and the solid/liquid contact angle (θ) are the critical

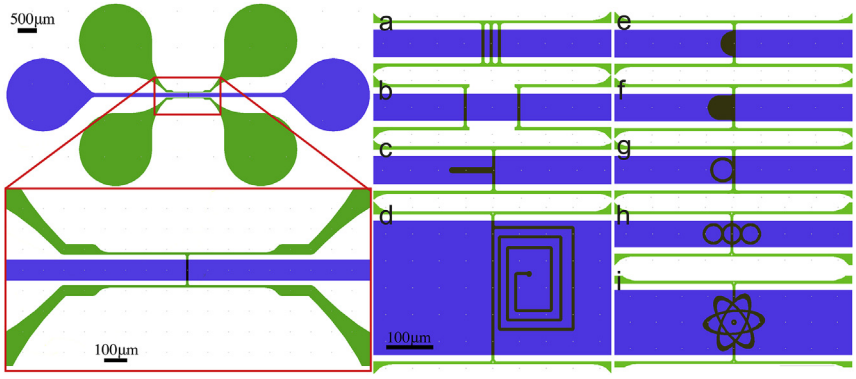

Fig. 4. Example of a lithography mask for a device with a simple straight open microfluidic geometry. The green features have a depth of 75 μm and the blue features of 35 μm, creating an open microfluidic channel of 40 μm in depth at the bottom of the channel indicated in blue. The reservoirs are 1 mm in radius. The channels start as 500 μm and tapers down to 50 μm and down to 10 μm close to the open microfluidic structure. The tapering of the channel increases the capillary pressure and assists in the successful capillary filling. (a–i) A few examples of more complicated shapes of the open microfluidics structures. Multiple channels (a,b), dead-end channels (c,d) patches (e,f) and closed loops/shapes(g,h,i) were investigated. (For interpretation of the references to colour in this figure legend, the reader is referred to the web version of this article.)

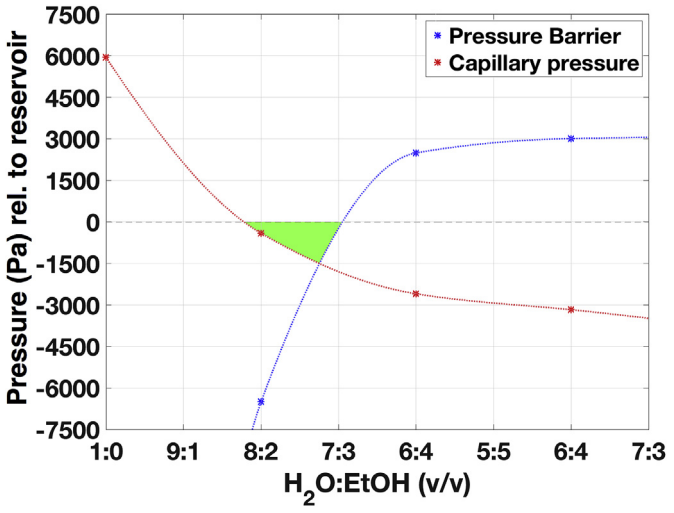

Fig. 5. Theoretical model of pressures. Blue shows the pressure barrier of the capillary valve (relative to reservoir pressure) and red shows the capillary pressure driving the filling of the open microfluidic feature, for different H_2O and EtOH mixtures. The operating range is shown with green color. (For interpretation of the references to colour in this figure legend, the reader is referred to the web version of this article.)

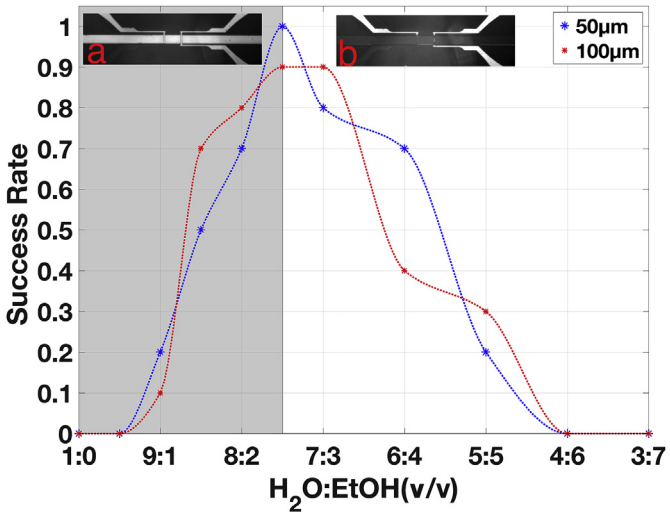

Fig. 6. Experimental results. For each water ethanol solution ten devices with a straight open microfluidic feature of 50 μm (blue color) and ten with a 100 μm (red color) open microfluidic were tested and the success rate for filling was recorded. If the device failed in the grey area it means that the open feature did not fill (a) and if it failed in the white area it means that the liquid front was not pinned at the capillary valve and the device flooded (b) as shown at the indent microscopy images. Once again the highest success rate is for solutions with H_2O:EtOH ratio between 8:2 and 7:3 that fits the theoretical model. (For interpretation of the references to colour in this figure legend, the reader is referred to the web version of this article.)

parameters that need to be controlled. On the one hand the liquid should be sufficiently wetting so that the condition for capillary filling and open microfluidics is met. On the other hand, the more wetting the liquid is (i.e. the lower the contact angle) and the lower the liquid/air interfacial tension, the lower the pressure barrier of the capillary valve. A low pressure barrier easily results in valve-breakthrough and flooding of the device. Contact angle and interfacial tension can be controlled by both surface and liquid properties. For the initial experiments to characterize the device operation we chose to vary the latter. Droplets of different mixtures of ethanol (EtOH) and water (H_2O) were introduced to the inlet reservoir of two different devices with a straight open microfluidic channel geometry (Fig. 4). The open microfluidic channels had a depth of 40 μm, a width of 10 μm and a length respectively of 50 μm and 100 μm. The capillary valves had a width of 10 μm and a height of 35 μm. Fig. 5 shows the theoretically predicted capillary valve pressure barrier (equation (9)) and the capillary pressure driving the filling of the open microfluidic feature for different H_2O and EtOH mixtures (equation (12)). The points on the graph were derived using the experimentally obtained values for contact angle and surface tension for different H_2O and EtOH mixtures reported in Refs. [19,20]. Dotted lines were added as a guide for the eye. Both pressures should be negative for a proper functionality of the device. If the pressure barrier has a positive value, then the device will flood and if the capillary pressure is positive then the open microfluidic feature will not fill. As shown in Fig. 5, according to the calculations both pressures are negative for solutions with a H_2O:EtOH ratio between 8:2 and 7:3(indicated by a green triangle) and with the optimum point with the lowest pressure (at the apex of the green triangle) at a H_2O:EtOH ratio of 7.25:2.75. In Fig. 6 the experimental results are shown. For each H_2O:EtOH ratio ten devices were tested and the success rate for filling (i.e. successful capillary pinning at the valve and successful filling of the open microfluidic feature) was recorded. If the device failed in the grey area, it means that the open feature did not fill (as shown in the microscopy image(a) of the inset) and if it failed in the white area it means that the liquid front was not pinned at the capillary valve and the device flooded (also see inset(b)). As theoretically predicted, the highest success rate was obtained for solutions with a H_2O:EtOH ratio between 8:2 and 7:3. Theoretically, the device should only work in this volume ratio range, but experimentally some devices were found to function outside this range. This can be explained by differences between devices due to fabrication. For example, we assume that the expansion angle of the capillary valve is 90°, while in reality a perfect right angle cannot be fabricated in PDMS and on the nanoscale corners will be rounded. In addition, it is known that the thickness of the SU-8 that is used for PDMS soft lithography can slightly vary depending on the position on the wafer [21]. Also, equation (9) that was used for the calculation of the pressure barrier is valid for a simple capillary stop valve with four liquid-solid interfaces, continuous bottom and top and an abrupt expansion on the side walls. In contrast, in our design the capillary valve has no solid bottom wall and hence has one less liquid-solid interface. This will alter the geometry of the meniscus, and hence the pressure barrier will be slightly different from the predicted one.

As was expected, the length of the open microfluidic structure did not affect the success rate of the device: when the filling condition is met (equation (11)) and the pressure at the meniscus is negative, then the open microfluidic structure will be passively filled independently of its length (see Fig. 6). As mentioned earlier the constant pressure at the liquid front results in a time-dependant flow velocity as the open microfluidic feature is filled, nevertheless the length of our features is small enough to neglect this phenomenon.

4.2. Method flexibility

The requirements for the capillary valve and the open microfluidic features are independent of each other, hence one can design various shapes of open microfluidics as long as the passive

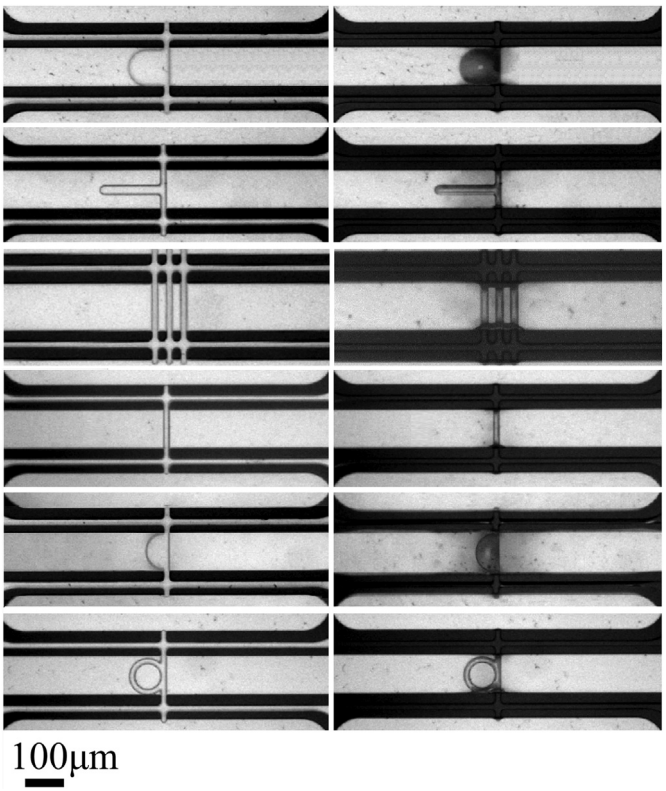

Fig. 7. Experimental results of various capillary patterns in the bottom channel wall prior to filling (left) and after filling with 7.5:2.5 H_2O:EtOH (right).

filling condition is met. Several different open microfluidics were tested in order to show the versatility of the proposed system in capillary patterning, and a few results are shown in Fig. 7. Bubble formation is a significant problem in filling microfluidic systems, but open microfluidics, where the air can simply escape, and which hence is insensitive to bubble formation, gives the opportunity for patterning dead end channels and loops which otherwise is impossible.

In practical applications it will not be easily possible to change the surface tension and contact angle by using solvent mixtures. However, surfactants can be used to control the surface tension and contact angle. Also, the contact angle can be controlled by changing the surface properties. For research purposes where PDMS is used, the contact angle can be controlled by plasma treatment and annealing at low temperature. By adjusting the plasma treatment time, we tuned the water contact angle of the PDMS to make the device suitable for filling with an aqueous solution, as we will show in the next section.

The most convenient way to obtain functioning devices for a wide variety of materials and solutions is by controlling the feature size and specifically the depth of the features, i.e. the height of the capillary valves and the depth of the open microfluidic channel. To illustrate the potential of this method, in Fig. 8 calculations for the capillary pressure in the open microfluidic structure and the pressure barrier of the capillary valve are plotted against the depth of each feature for two different solutions, that vary in contact angle and surface tension. The width of both features is set to 10 μm. Once again both pressures are required to be negative, so that the necessary depths of the features can be obtained from the graphs. Similar graphs can for example be made for different feature widths. With such analyses, one can tailor the device for any

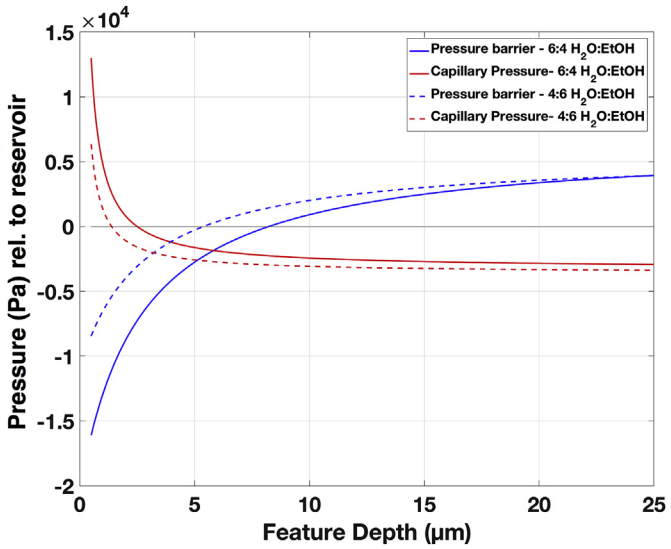

Fig. 8. Capillary barrier pressure and capillary filling pressure vs feature depth for two different solutions. Both pressures are required to be negative.

specific material, solution and application.

4.3. Antibody patterning with an aqueous solution

We demonstrate the practical usefulness of our method by applying it for capillary patterning of antibodies for immunodetection. As mentioned earlier we tuned the contact angle of the PDMS chips, via O_2 plasma treatment and low temperature annealing, so the proper functionality of the device was ensured for aqueous solutions. We show that is possible to pattern after bonding, hence in a closed chip, which otherwise is cumbersome.

In Fig. 9 the results are shown. After the capillary patterning we demonstrated the intact functionality of the antibodies by flushing the channels with fluorescent antigen. The results prove that the simple technique based on capillary phenomena enables patterning of antibodies in closed chips, with subsequent antigen immunodetection. The patterning freedom offered by the method is evidenced by successful coating of simple straight channels (Fig. 9a–c), to more complex shapes (Fig. 9d–i). The pattern resolution (i.e. feature size) attainable by this method will depend on the limits of microfabrication, where standard photolithography can create reproducible channels with widths down to 5 μm.

Our examples use PDMS only to demonstrate the method. As mentioned in the introduction, in future this technique is meant for use in closed glass or plastic chips that are suitable for diagnostic devices. One further point that needs consideration in the final devices is closing the 3D capillary valve channel exits, since the sample solution will leak out via these channels. An easy solution to this problem is the blocking of the 3D valve reservoirs prior to the introduction of antigen e.g. by glue. The trapped air in the channels will then allow only minute volumes to enter the capillary valve channels.

5. Conclusion

The use of 3D capillary valves has been investigated for capillary patterning in closed microchips. We theoretically described the functionality of the system for selective filling of parts of a closed microfluidic structure and the experimental results adequately fit the proposed theoretical model. The model can be used as a design tool for tailoring 3D valves for various applications, solutions and

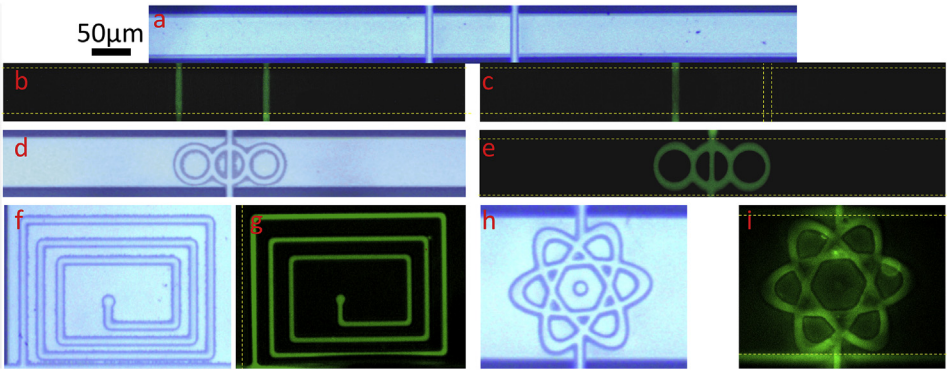

Fig. 9. Microscopy images of antibody antigen reactions after antibody patterning. Channel walls are marked with yellow dashed lines a) Bright field image of a chip with two straight channels for antibody coating. b,c) Fluorescent imaging of the chip with two(b) and one(c) channels coated with antibody and incubated with fluorescent antigen. d,f,h) Bright field images of more complex patterns. e,g,i) Fluorescent images after antibody coating and fluorescent antigen incubation. Scale bar in upper left corner. (For interpretation of the references to colour in this figure legend, the reader is referred to the web version of this article.)

materials as long as the contact angle and surface tension are known. In addition, we demonstrate that the method can be used to create a simple immunodetection device by demonstrating a passive antibody pattering of various shapes in a closed chip followed by antigen binding. The technique can find various applications such as capillary patterning of phase change materials e.g. hydrogels and local surface functionalization in closed chips.

Acknowledgements

This work was supported and funded by Horizon 2020 Framework Programme of the European Union under the project H2020-PHC-634013 (PHOCNOSIS).

Appendix A. Supplementary data

Supplementary data related to this article can be found at https://doi.org/10.1016/j.aca.2017.11.055.

References

[1] T.M. Squires, R.J. Messinger, S.R. Manalis, Making it stick: convection, reaction and diffusion in surface-based biosensors, Nat. Biotechnol. 26 (2008) 417–426, https://doi.org/10.1038/nbt1388.
[2] S. Cesaro-Tadic, G. Dernick, D. Juncker, G. Buurman, H. Kropshofer, B. Michel, C. Fattinger, E. Delamarche, High-sensitivity miniaturized immunoassays for tumor necrosis factor alpha using microfluidic systems, Lab. Chip 4 (2004) 563–569, https://doi.org/10.1039/b408964b.
[3] A. Bernard, J.P. Renault, B. Michel, H.R. Bosshard, E. Delamarche, Microcontact printing of proteins, Adv. Mater 12 (2000) 1067–1070, https://doi.org/10.1002/1521-4095(200007)12:14<1067::Aid-Adma1067>3.0.Co;2-M.
[4] T. Snabe, G.A. Røder, M.T. Neves-Petersen, S. Buus, S.B. Petersen, Oriented coupling of major histocompatibility complex (MHC) to sensor surfaces using light assisted immobilisation technology, Biosens. Bioelectron. 21 (2006) 1553–1559, https://doi.org/10.1016/j.bios.2005.06.010.
[5] J. Kim, J. Kim, Y. Shin, S. Song, J. Lee, Rapid prototyping of multifunctional microfluidic cartridges for electrochemical biosensing platforms, Sensors Actuators B Chem. 202 (2014) 60–66, https://doi.org/10.1016/j.snb.2014.05.009.
[6] F. Saharil, C.F. Carlborg, T. Haraldsson, W. van der Wijngaart, Biocompatible "click" wafer bonding for microfluidic devices, Lab. Chip 12 (2012) 3032, https://doi.org/10.1039/c2lc21098c.
[7] A.H. Diercks, A. Ozinsky, C.L. Hansen, J.M. Spotts, D.J. Rodriguez, A. Aderem, A microfluidic device for multiplexed protein detection in nano-liter volumes, Anal. Biochem. 386 (2009) 30–35, https://doi.org/10.1016/j.ab.2008.12.012.
[8] J.C.T. Eijkel, A. van den Berg, Young 4ever—the use of capillarity for passive flow handling in lab on a chip devices, Lab. Chip 6 (2006) 1405–1408, https://doi.org/10.1039/B613839J.
[9] E. Delamarche, D. Juncker, H. Schmid, Microfluidics for processing surfaces and miniaturizing biological assays, Adv. Mater 17 (2005) 2911–2933, https://doi.org/10.1002/adma.200501129.
[10] D. Juncker, H. Schmid, U. Drechsler, H. Wolf, M. Wolf, B. Michel, N. De Rooij, E. Delamarche, Autonomous microfluidic capillary system, Anal. Chem. 74 (2002) 6139–6144, https://doi.org/10.1021/ac0261449.
[11] B. Gumuscu, J.G. Bomer, A. van den Berg, J.C.T. Eijkel, Large scale patterning of hydrogel microarrays using capillary pinning, Lab. Chip 15 (2015) 664–667, https://doi.org/10.1039/C4LC01350F.
[12] E. Yildirim, S.J. Trietsch, J. Joore, A. van den Berg, T. Hankemeier, P. Vulto, Phaseguides as tunable passive microvalves for liquid routing in complex microfluidic networks, Lab. Chip 14 (2014) 3334, https://doi.org/10.1039/C4LC00261J.
[13] P.F. Man, C.H. Mastrangelo, M.A. Burns, D.T. Burke, Microfabricated capillarity-driven stop valve and sample injector, in: Proc. MEMS 98. IEEE. Elev. Annu. Int. Work. Micro Electro Mech. Syst. An Investig. Micro Struct. Sensors, Actuators, Mach. Syst. (Cat. No.98CH36176), 1998, pp. 45–50, https://doi.org/10.1109/MEMSYS.1998.659727.
[14] B.P. Casavant, E. Berthier, A.B. Theberge, J. Berthier, S.I. Montanez-Sauri, L.L. Bischel, K. Brakke, C.J. Hedman, W. Bushman, N.P. Keller, D.J. Beebe, Suspended microfluidics, Proc. Natl. Acad. Sci. 110 (2013) 10111–10116, https://doi.org/10.1073/pnas.1302566110.
[15] T.S. Leu, P.Y. Chang, Pressure barrier of capillary stop valves in micro sample separators, Sensors Actuators A Phys. (2004) 508–515, https://doi.org/10.1016/j.sna.2004.02.036.
[16] B. Hagmeyer, F. Zechnall, M. Stelzle, Towards plug and play filling of microfluidic devices by utilizing networks of capillary stop valves, Biomicrofluidics 8 (2014), https://doi.org/10.1063/1.4896063.
[17] J. Berthier, K.A. Brakke, E. Berthier, Open Microfluidics, Scrivener Publishing, 100 Cummings Center, 2016. Suite 541J Beverly, MA 01915-6106.
[18] D.B. Weibel, W.R. DiLuzio, G.M. Whitesides, Microfabrication meets microbiology, Nat. Rev. Microbiol. 5 (2007) 209–218, https://doi.org/10.1038/nrmicro1616.
[19] H. Cao, C. Amador, X. Jia, Y. Ding, Capillary dynamics of water/ethanol mixtures, Ind. Eng. Chem. Res. 54 (2015) 12196–12203, https://doi.org/10.1021/acs.iecr.5b03366.
[20] H. Mishra, A.M. Schrader, D.W. Lee, A. Gallo, S.Y. Chen, Y. Kaufman, S. Das, J.N. Israelachvili, Time-dependent wetting behavior of PDMS surfaces with bioinspired, hierarchical structures, ACS Appl. Mater. Interfaces 8 (2016) 8168–8174, https://doi.org/10.1021/acsami.5b10721.
[21] A. Mata, A.J. Fleischman, S. Roy, Fabrication of multi-layer SU-8 microstructures, J. Micromech. Microeng. 16 (2006) 276–284, https://doi.org/10.1088/0960-1317/16/2/012.